Analysis of d–d Transitions in $[Cr(CN)(NH_3)_5]^{2+}$ as Inferred from Polarized Optical Spectra and Angular Overlap Model Calculations

Akio Urushiyama,* Mutsuyoshi Itoh, and Thomas Schönherr†

Department of Chemistry, College of Science, Rikkyo University, Nishiikebukuro 3, Toshima-ku, Tokyo 171

†Institut für Theoretische Chemie, Heinrich-Heine-Universität Düsseldorf, Universitäts Straße 1, 40225 Düsseldorf, Germany

(Received August 11, 1994)

The polarized single-crystal absorption spectra of $[Cr(CN)(NH_3)_5]Cl(ClO_4)$ were measured for interconfigurational quartet ($t_{2g}^3 \rightarrow t_{2g}^2 e_g$) and intraconfigurational doublet transitions ($t_{2g}^3 \rightarrow t_{2g}^3$). The band splittings of the spin-allowed transitions, $^4A_{2g} \rightarrow {}^4T_{2g}, {}^4T_{1g}$, were derived to 600—1000 cm^{-1} from a Gaussian band deconvolution of the σ and π spectra. At low temperature (77 K), more than 45 sharp bands could be detected in the intercombination band region of the lowest doublets (^2E_g, $^2T_{1g}$), which were completely assigned to the five possible zero-phonon transitions and corresponding vibronic sidebands. The vibrational frequencies due to the electronic ground state were obtained from the infrared spectrum and by measuring the emission lines under resonant excitation, providing us with a sufficient data base for a normal coordinate treatment of the pentaamminecyano cation. The d-energy level scheme is rationalized using the angular overlap model (AOM). Geometric parameters were obtained from an X-ray analysis of the chloride–perchloride salt, which shows a cation of approximately $4mm$ (C_{4v}) site symmetry, consistent with a linearly coordinated cyano group. The AOM parameters evaluated for the CN^- ligand show strong σ-antibonding (e_σ=ca. 7500 cm^{-1}) together with unusually larger π-bonding (e_π=ca. −900 cm^{-1}), which both contribute to the extremely high value of the respective ligand field parameter Dq. The large splitting of the lowest doublet state, ^2E_g (O_h), has been shown to originate from a low-symmetry effect in the treatment of interelectronic repulsion. The attributed tetragonal orbital expansion parameter (τ=0.99) was calculated to be similar to values recently obtained for related pentaammineaniono complexes.

The ligand field states of pentaammineaniono complexes of chromium(III) have been thoroughly studied owing to their interesting photochemical behavior. In his pioneering work, Schläfer[1] suggested the involvement of the lowest excited state in light-induced racemization and substitution reactions. By examining the band shapes of spin-forbidden transitions in the luminescence spectra, Forster[2] classified a series of mono- and disubstituted ammine complexes into ^2E_g and $^2T_{1g}$ emitters; the experimental data were interpreted in terms of the angular overlap model (AOM)[3] with special emphasis placed on the particular metal-ligand interactions. In this field, the exceptionally large splitting of the lowest excited state, $^2E_g(O_h)$, observed in many tetragonal Cr(III) complexes, has been the object of a long-standing discussion.[4—7] For a chromium (III) complex, which contains hard (NH_3) and soft (CN^-) ligands simultaneously, a substantial analysis of ligand field states is not yet available. The nature of the cyanide ligand concerning its σ- and π-bonding interaction is also not clear, though a π-acceptor behavior has recently[8,9] been assumed. Otherwise, the ligand field parameter $10Dq$ (CN^-) that represents the energy difference between the t_{2g} and e_g orbitals in cubic environments is well known to be extremely large, showing CN^- at the end of the spectrochemical series. The specific bonding properties to a distinct metal ion, however, can not be derived from this parameter. On the other hand, an analysis of low-symmetry band splittings, when rationalized in terms of the angular overlap model (AOM), can provide such information. This has recently been demonstrated for a series of non-cubic chromium(III) complexes which contain various different ligands as ammine, halides, oxalate, pyridine, and/or acetylacetonate.[7,10,11] Accordingly, we attempted to grow single crystals. We present here structural data and a complete AOM analysis of detailed polarized d–d transitions in pentaamminecyanochromium(III).

Experimental

Preparation of the Compounds. Yellow solids of $[Cr(CN)(NH_3)_5]Cl_2$ and $[Cr(CN)(NH_3)_5](ClO_4)_2$ were prepared according to the literature.[9] The measured UV-vis absorption maxima were in good agreement with the values

reported there. The deuterated derivatives were obtained by recrystallizing twice from a D_2O solution. The IR bands in the 3200—3400 cm^{-1} region, which are due to (N–H) strechings vibrations, were completely shifted into the 2600—2800 cm^{-1} region by this deuteration. The addition of perchloric acid (70%) to a saturated aqueous solution of the chloride yields chloride–perchlorate salt, $[Cr(CN)(NH_3)_5]Cl(ClO_4)$. From this salt we could obtain single-crystals suitable for low-temperature polarized absorption measurements by an overnight standing of a saturated solution in a refrigerator (5 °C). For an X-ray investigation, crystals were selected from the same crop. Unfortunately, well-shaped single crystals suitable for optical measurements could not be obtained for the analogous deuterated compounds.

Found: C, 4.06; H, 5.06; N, 28.16%. Calcd for $[Cr(CN)(NH_3)_5]Cl(ClO_4)$: C, 4.03; H, 5.07; N, 28.19%.

Spectroscopic Measurements: The single-crystal polarized absorption spectra were measured in the spin-allowed region (18000—32000 cm^{-1}) using a Hitachi model EPS-3T spectrometer and specially designed micro-spectroscopic equipment. The light beam passed through a Rochon quartz polarizer and was then condensed by two concave mirrors onto a pinhole (ϕ=0.1 mm) in an indium plate where a thin crystal of $[Cr(CN)(NH_3)_5]Cl(ClO_4)$ (face=0.48×0.15 mm^2, thickness=0.05 mm) was placed using a small amount of silicone grease. The orientation of the four-fold rotation axis of the tetragonal crystal system was rectangular to the direction of the light propagation, so that the σ and π polarized spectra could be obtained. Complete covering of the pinhole by the sample crystal is necessary. The reference beam was appropriately attenuated so that the absorbance was adjusted to zero for the longer wavelength region (<14000 cm^{-1}) where the crystal does not absorb.

Measurements in the intercombination band region (14000—16500 cm^{-1}) were performed with a Jobin-Yvon U-1000 monochromator by a method similar as described in a previous paper.[13] A well-grown plate (0.48×0.70×0.125 mm^3) of a single crystal of $[Cr(CN)(NH_3)_5]Cl(ClO_4)$ was fixed into a small pinhole of an indium plate with the light propagation again perpendicular to the tetragonal axis, so that the optical thickness was 0.48 mm in this case of the sample setting. A small amount of non-transparent oil-compound was used to ensure complete blocking from stray light. The fixed sample was then placed into the narrow gap of the edges of two flexible light guides, and completely immersed in a liquid-nitrogen dewar (10 liters). A small piece cut from a film polarizer, which was placed just upon the sample crystal, served for light polarization even at liquid-nitrogen temperature. The passed light was monitored by a photon-counting apparatus (Hamamatsu Photonics C767). All of the measurements were performed under an optical resolution of about 3 cm^{-1}. The reproducibility of the spectra was proved during an acquisition time of over one week.

Some very weak bands in the higher vibronic region of spin–forbidden transitions between 16500 and 19000 cm^{-1} were detected by non-polarized measurements. For these measurements about 100 mg of granular crystals were filled into a small aluminum pipe (ϕ=3 mm) which was attached at both ends by the light pipes. In order to also maintain a sufficiently high light transparency at the liquid-nitrogen temperature a small amount of nujol was advantageously mixed with the crystals. The apparent thickness of the probe could be up to 3 mm, while retaining sufficient transparency for measurements under a resolution of 10 cm^{-1}. For the absorption band at 18058 cm^{-1} (No. 39 in Table 1), for example, the molar extinction coefficient (ε) could be estimated to be as small as 0.016 based on the apparent optical length within the aluminum pipe.

The emission spectra were obtained by laser excitation using the spectral equipment previously described.[7] A resonant spectrum, which shows the best resolved vibronic fine-structure, was obtained by tunable dye-laser excitation directly into the zero-phonon line of the lowest electronic state, ^2E_g (O_h). The UV-vis solution spectra were measured by a Hitachi model-3400 spectrometer. Infrared spectra were recorded with a Perkin–Elmer 1600 FTIR spectrometer (4000—600 cm^{-1}) and in the far-infrared region with a Hitachi IR-F instrument in nujol phase.

X-Ray Analysis: An essential part of the crystal structure measurements was performed by a four-circle automated diffractometer (Ragaku AFC-5). The crystal of $[Cr(CN)(NH_3)_5]Cl(ClO_4)$ belongs to a tetragonal system. The cell constants are $a=b$=772.9 pm and c=976.5 pm with two formula units in the cell (Z=2). The calculated density of D_c=1.86 g cm^{-3} corresponds exactly to the measured value (D_m=1.86 g cm^{-3}). The space group was identified as being either $P4/n$ or $P4/nmm$. The intensity data collection was performed using a ω–2θ scan mode ($2° < 2\theta < 55°$). After applying the absorption correction of North et al.,[13] a total of 524 independent reflections were used to solve the structure. All of the computational work was performed using the a HITAC 682H computer at the Computer Center of the University of Tokyo using the universal progarm system for X-ray crystallogrpaphy, UNICSIII (library program). An ordinary heavy-atom method of analysis revealed that the perchrolate anions were disorderedly oriented in the cell, so that the R factor did not decrease sufficiently, even at the final stage of a block-diagonal least-square refinement ($P4/nmm$: R=0.12), in which, for the perchrlate anion, the octahedrally coordinated oxygen atoms (tetragonally distorted: 153 pm (equatorial), 134 pm (axial)) with appropriately reduced multiplicities were assumed to exist around the chlorine atom, which is located at x/a=0.0, y/b=0.0, z/c=0.5. However, the results (even at this stage) were quite reasonable, as far as the structure of the complex cation was concerned, i.e., 199 pm (Cr–N), 194 pm (Cr–C), and 111 pm (C–N). Essentially a similar crystal structure was obtained by analyses assuming either the $P4/n$ or the $P4/nmm$ space group. The N–C–Cr–N(*trans*) sequence of the complex cation is placed in the line through x/a=0 and y/b=0 which has the symmetry $\bar{4}$ when the space group $P4/n$ is assumed. This direction is coincident with the tetragonal crystal c-axis. In the case of $P4/nmm$, on the other hand, the molecular symmetry $\bar{4}m2$ is present.

Normal Coordinate Analysis: Due to the actual C_{4v} point symmetry the 18 normal vibrations which correspond to the $[Cr(CN)N_5]$ chromophore transform as $5a_1+2b_1+b_2+5e$. Symmetry arguments predict that only the fundamentals of a_1 and e symmetry will induce a considerable transition intensity by the electric-dipole mechanism. In view of the results concerning similar pentaammine complexes, we can assign the peaks at 475, 459, and 431 cm^{-1} in the infrared spectrum to $\sigma(Cr–NH_3)$ stretching vibrations of a_1 and e symmetry, whereas the weak feature appearing

Table 1. Vibrational Frequencies (ν/cm^{-1}) or $[Cr(CN)(NH_3)_5]Cl_2$ and the Deuterated Derivative (See Text)

	Observed			Calculated		
Notation	H	D	H/D	H	D	H/D
σ(N–H)$_{as}$	3335	2473	1.35	3301	2536	1.30
	3255					
σ(N–H)$_s$	3188	2371	1.34			
	3148	2328	1.35	3130	2289	1.37
σ(C–N)	2130	2140	1.00	2083	2083	1.00
δ(H–N–H)$_s$	1637	1191	1.37	1631	1251	1.30
	1617					
	1606			1295	937	
δ(H–N–H)$_{as}$	1312	1010	1.29	1104	1106	
				1004	936	
ρ(Cr–NH$_3$)	724	586	1.24	761	854	
				747	583	1.28
$\nu_1(a_1)$: σ(Cr–N)$_{ax}$, σ(Cr–C)	459	427	1.07	481	460	1.05
$\nu_2(a_1)$: σ(Cr–N)$_{eq}$	431	400	1.08	398	365	1.08
$\nu_3(b_1)$: σ(Cr–N)$_{eq}$	420	390	1.08	372	342	1.09
$\nu_4(e)$: σ(Cr–N)$_{eq}$	475	440	1.08	496	468	1.06
$\nu_5(a_1)$: σ(Cr–C), σ(Cr–N)$_{ax}$	359	347	1.03	352	336	1.05
$\nu_6(e)$: δ(Cr–C–N), δ(N–Cr–C)	342	338	1.01	346	340	1.02
$\nu_7(e)$: δ(N–Cr–N)	280	250sh	1.12	264	232	1.14
$\nu_8(e)$: δ(N–Cr–N)	250	227	1.10	252	225	1.12
$\nu_9(e)$: δ(N–Cr–N)	225			235	214	1.10

Force constants (H, F (Urey–Bradley type)/mdyn Å): K(Cr–N)=3.40, K(Cr–C)=3.20, K(C–N)=12.00, K(N–H)=4.00, H(N–Cr–N)=0.40, F(N–Cr–N)=0.20, H(N–Cr–C)=0.40, F(N–Cr–C)=0.20, H(Cr–N–H)=0.20, F(Cr–N–H)=0.40, H(Cr–N–H)=0.20, F(H–N–H)=0.60, Cr–C–N bending=0.15 mdyn Å, NH_3 torsion=0.1 mdyn Å.

in this region is probably due to the respective b_1 mode (420 cm^{-1}). These bands all show isotopic shifts on deuteration, as is typically observed for related complexes showing a ratio (νH/νD) of between 1.07 and 1.11.[6] Since bending modes of types $\delta(H_3N–Cr–NH_3)$ and $\delta(H_3N–Cr–CN)$ are expected at frequencies lower than 300 cm^{-1}, the two medium-strong bands at around 350 cm^{-1}, which show significantly smaller isotopic shifts, can be reasonably assigned to the σ(Cr–CN) streching (a_1) and δ(Cr–C–N) bending (e) vibrations.

The given assignments were confirmed by a full normal coordinate treatment which also considered the 15 hydrogen atoms of the ammine groups. The calculations were performed using the familiar GF matrix method of Wilson[15] and library routines of the Computer Center of the University of Tokyo. The programs (BGLZ and LSMB)[16] were transformed for installation into a personal computer (NEC PC-9801VM2), revising mainly on input and output procedures. The geometrical parameters of the hydrogens were appropriately assumed to retain a maximal symmetry of C_s for the complex. Table 1 collects experimental data with the calculated frequencies obtained by means of a Urey–Bradley force field.

Results and Discussion

Optical Spectra. A) Spin-Allowed Transitions: The absorption spectrum of the pentaamminecyano complex shows a band pattern like that typically observed for octahedrally coordinated chromium(III) compounds with two spin-allowed bands in the UV-vis spectral region, which are due to the transitions $^4A_{2g}\rightarrow{}^4T_{2g}$ and $^4A_{2g}\rightarrow{}^4T_{1g}$. The tetragonal contribution of the cyanide ligand to the ligand field potential causes an optical anisotropy in the present compounds. This is illustrated in Fig. 1A, showing slightly different band shapes for σ- and π-polarization in the single-crystal absorption spectra of $[Cr(CN)(NH_3)_5]Cl(ClO_4)$. As expected from the similar positions of ammonia and cyanide in the spectrochemical series, a splitting of the quartet bands can not be detected. However, a deconvolution procedure using a Gaussian least-squares fit on the experimental band pattern yielded maxima at ca. 21600 cm^{-1}, ca. 22280 cm^{-1} and ca. 28100 cm^{-1}, ca. 29050 cm^{-1}, for the tetragonal split levels of $^4T_{2g}$ ($^4B_2$, $^4E^a$) and $^4T_{1g}$ ($^4A_2$, $^4E^b$), respectively (Figs. 1B and 1C). This result is supported by arguments which consider static and vibronic selection rules for the underlying C_{4v} symmetry of the chromophore. For example, considering π-polarizaition (x,y), electric-dipole transitions from the ground state $^4B_1(C_{4v})$ are allowed only into the orbitally degenerate $^4E(C_{4v})$ states, because in this case the direct product of the respective irreducible representations contains a totally symmetric term:

$$B_1 \times E(x,y) \times E = A_1 + \quad (1)$$

Transitions into either the $^4B_2(C_{4v})$ or $^4A_2(C_{4v})$ excited states, otherwise, require a vibronic coupling

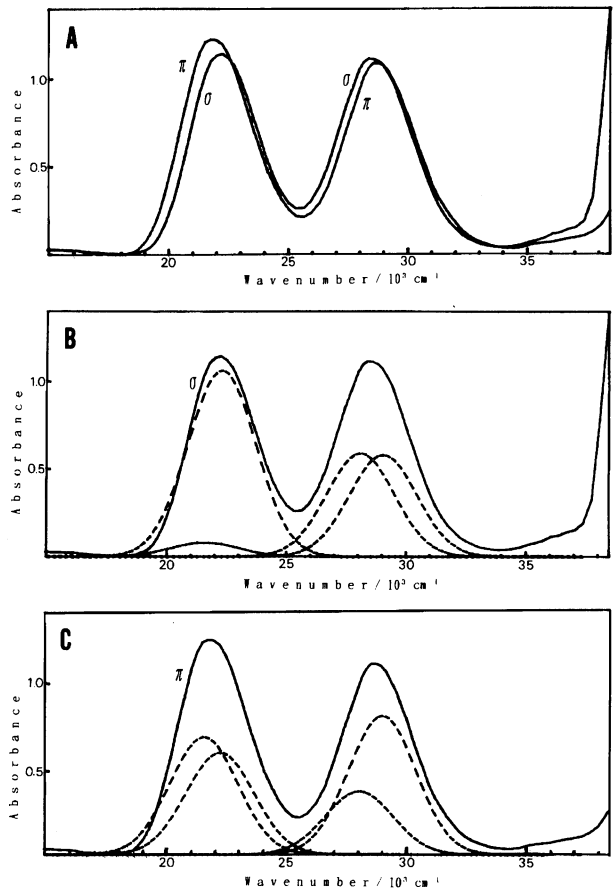

Fig. 1. Polarized absorption spectra of $[Cr(CN)(NH_3)_5]Cl(ClO_4)$ in the spin-allowed transition region at room temperature (A). Gaussian analyses of the ligand filed absorption bands are given of the σ- (B) and π-spectrum (C). The analyses were performed assuming the same value of half-width, which was optimized to be 3350 cm^{-1}, for all four band components in the σ- and π-spectrum.

mechanism which usually causes less intense bands, due to large energy denominators that appear in the corresponding matrix elements.[17] Static and dynamic selection rules for spin-allowed transitions from the $^4B_1(C_{4v})$ ground state are collected in Table 2. It follows that transitions into any quartet state can gain vibronic intensity by promoting modes of proper symmetry if the electric vector of the propagating light is orientated along the tetragonal axis (π-polarization). In σ-polarization, on the other hand, both mechanisms can not account for the transition $^4B_1 \rightarrow {}^4B_2$ when the molecular vibrations of $[CrN_5CN]$ moiety are considered, because none of them transform as a_2 (see above). This behavior is indeed reflected by our band deconvolution, showing only a very small feature at the low-energy side of the first quartet band (Fig. 1B). Considering also the higher intensity of the second component of $^4T_{1g}$ in the σ-spectrum, we can conclude the level ordering.

$$^4B_2 < {}^4E^a. \quad (2)$$

The location of the $^4T_{2g}$ split levels is also consistent with conventional ligand filed theory (LFT), which predicts for tetragonal complexes the corresponding transition energies as calculated from the familiar relations:[17]

$$^4B_1 \rightarrow {}^4B_2 \quad \text{corresponds} \quad 10Dq(NH_3) \quad (3)$$

$$^4E^a \rightarrow {}^4B_2 \quad \text{corresponds} \quad 35/4Dt \quad (4)$$

$$Dt = 2/7(Dq(CN) - Dq(NH_3)) \quad (5)$$

Therefore, we expect from the position of the ammonia ($Dq(NH_3) = 2160$ cm^{-1}) and cyanide ($Dq(CN) = 2630$ cm^{-1}) ligands in the spectrochemical series[17] a splitting of around +1000 cm^{-1} that is in qualitative agreement with the value obtained by means of the band-fit procedure. The splitting of the second quartet band depends, on the other hand, on a second parameter (Ds) which cannot be evaluated within the parametrizaiton of the LFT from cubic quantities alone. We discuss this splitting later in the context of our AOM calculations.

B) Spin-Forbidden Transitions: Intraconfigurational $t_{2g}^3 \rightarrow t_{2g}^3$ transitions in chromium(III) complexes, when measured at sufficiently low temperatures, usually give rise to a series of sharp lines in the long-wavelength part of the visible absorption spectrum. Figure 2 shows the crystal absorption spectra of $[Cr(CN)(NH_3)_5]Cl(ClO_4)$ in σ- and π-polarization measured at 78 K; an unpolarized spectrum of very weak transitions in the higher energy part is given in Fig. 3. Deuterium shifts of the vibronic lines are depicted in Fig. 4 for the respective chloride salts. A luminescence spectrum obtained under resonant excitation is shown in Fig. 5. The numerical values of the sharp absorption lines are collected in Table 3 together with corresponding assignments which correlate with data obtained from infrared and emission spectra.

In order to give an impression of the complex assignment problem for the spin-forbidden transitions we discuss in the following some features in more detail. For example, the characteristic intense sharp lines 1 and 4 (Fig. 2), both of which have counterparts in the non-resonant emission spectrum (which is not given here), are readily identified with the zero-phonon transitions into the split levels of $^2E_g(O_h)$. This doublet state is

Table 2. Electric-Dipole Selection Rules for Spin-Allowed Transitions in C_{4v} Symmetry

$(^4A_{2g})$		$(^4T_{2g})$		$(^4T_{1g})$	
B_1		B_2	E^a	A_2	E^b
π-Polarization	Static	—	x	—	x
	Vibronic	e	a_1, b_1, b_2	e	a_1, b_1, b_2
σ-Polarization	Static	—	—	—	—
	Vibronic	(a_2)	e	b_2	e

Vibrational modes of a_2 symmetry does not occur for the $[Cr(CN)N_5]$ moiety.

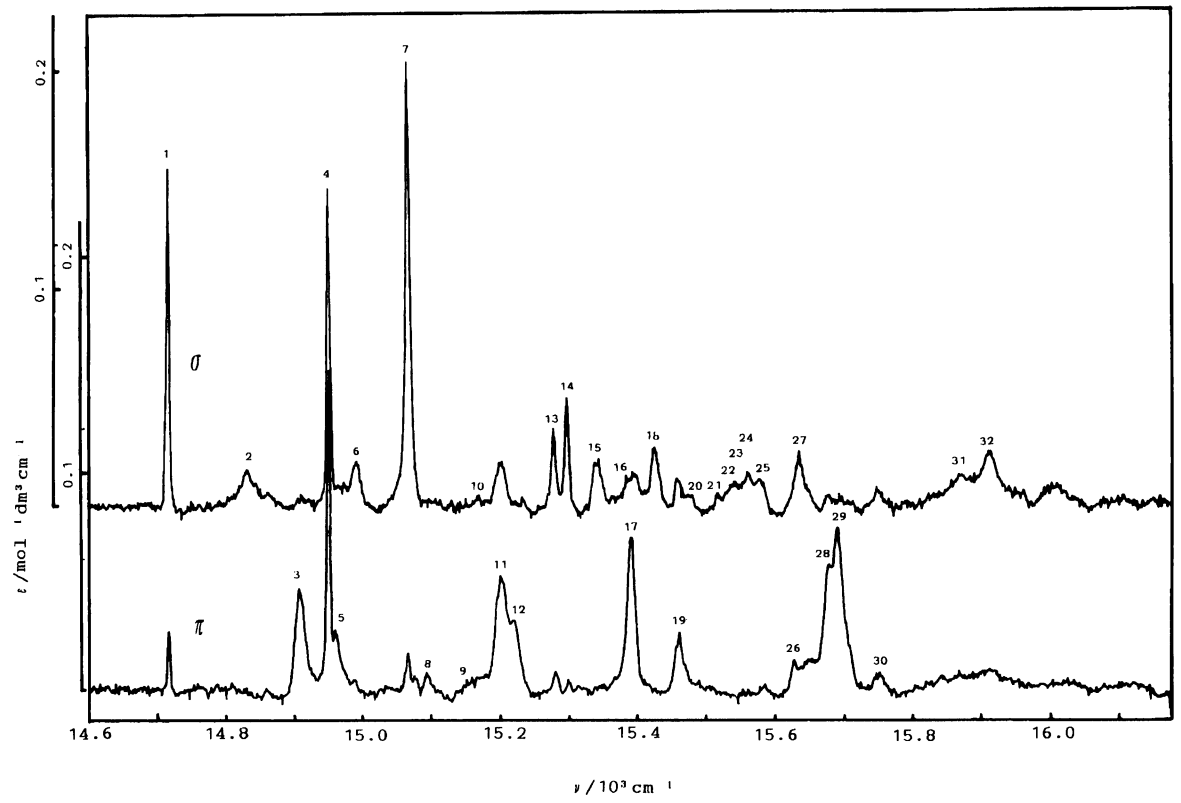

Fig. 2. Polarized absorption spectra of $[Cr(CN)(NH_3)_5]Cl(ClO_4)$ in the region of t_{2g}^3 intraconfigurational transitions measured at 78 K.

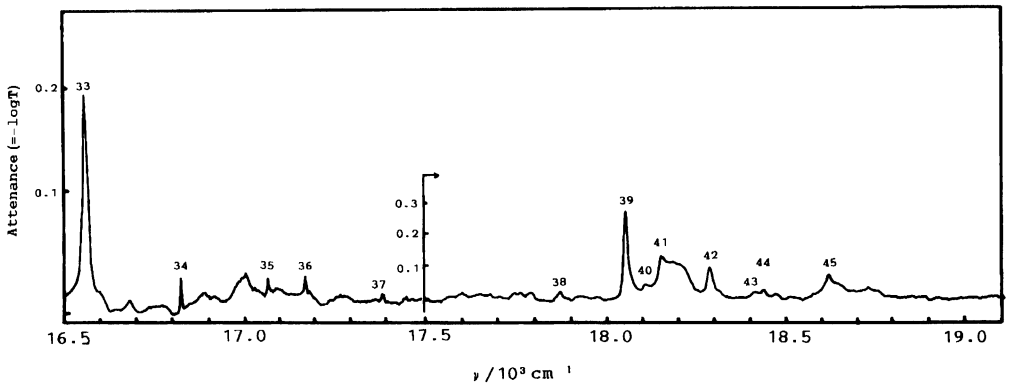

Fig. 3. Absorption spectrum of microcrystalline $[Cr(CN)(NH_3)_5]Cl(ClO_4)$ in the higher energy part of vibronic spin-forbidden transitions at 78 K.

split by the tetragonal ligand field into $^2A_1$ and $^2B_1$, or the Kramers doublets Γ_6 and Γ_7, respectively, when the spin-orbit coupling is taken into account. These assignments are supported by the appearance of the intense satellites 7 and 14, which differ from the respective origin by $\nu_5(a_1)=351$ cm^{-1}. A corresponding sideband due to this σ(Cr–C) stretching mode is located at 14338 cm^{-1} in the emission spectrum, likewise (cf. Fig. 5). Further correspondences are also obtained for several other frequencies, which are assigned based on an analysis of the infrared and/or emission data. For example, the rocking modes ρ(Cr–NH_3) appear as quite intense vibronic sidebands of the lowest origin, which turns out to be $^2A_1$ (see next section). These lines (15—20) have adequate counterparts in the region of lines 26—29 due to corresponding sidebands of the higher $^2E_g(O_h)$ split level ($^2B_1$). In fact, towards higher energy most features in the intercombination band spectrum can be interpreted in terms of a vibrational structure (fundermentals and combinations) based upon two zero-phonon transitions. Otherwise, the sharp line (13), which is located 569 cm^{-1} above line 1, should certainly belong to one of the three split levels of $^2T_{1g}(O_h)$. This assignment is established by the following arguments:

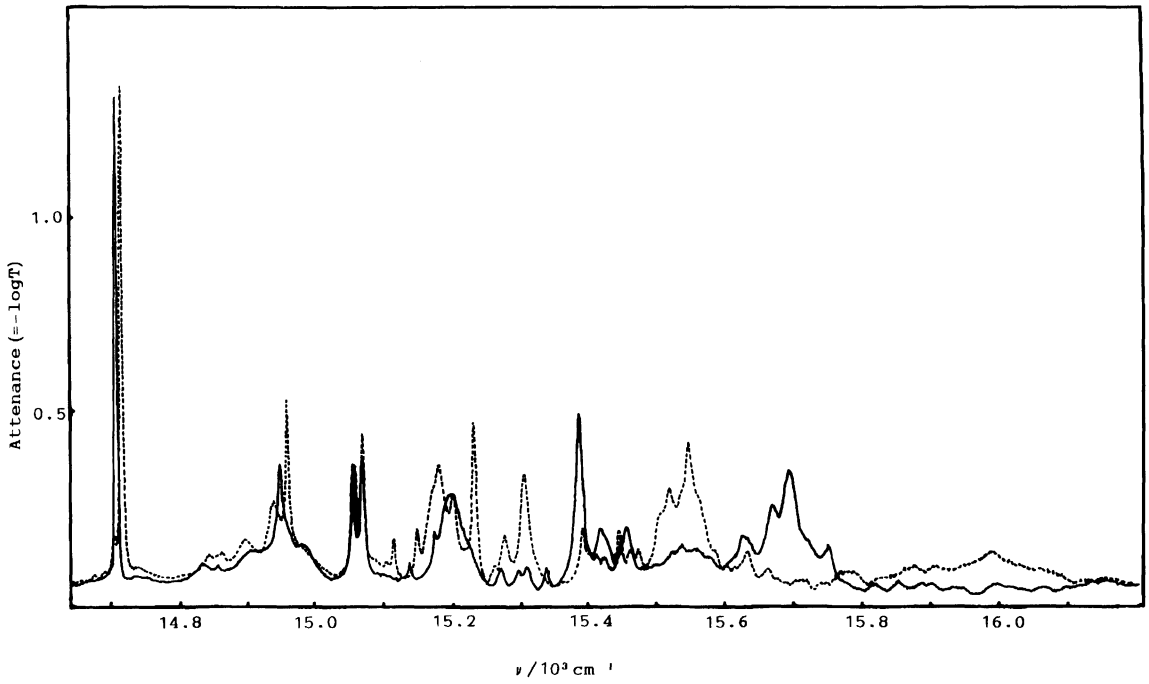

Fig. 4. Crystal absorption spectra of $[Cr(CN)(NH_3)_5]Cl_2$, (solid line) and the deuterated derivative (dotted line) in the intraconfigurational transition region at 78 K.

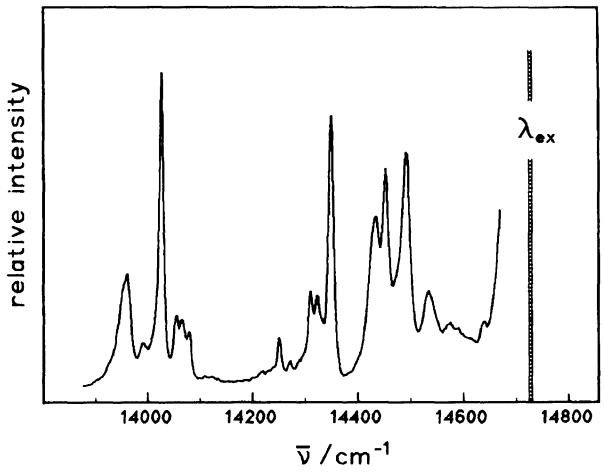

Fig. 5. Low-temperature (1.9 K) emission spectrum of microcrystalline powder of $[Cr(CN)(NH_3)_5]Cl_2$ obtained under resonant excitation (λ_{ex}=679 nm).

(i) An identification of this line with a vibronic sideband of $^2A_1$ fails because an intramolecular vibration around 570 cm^{-1} does not exist;

(ii) There is no line corresponding to (13) in the luminescence spectrum;

(iii) An assignment of (13) to a sideband of $^2B_1$ would require a vibrational frequency of 328 cm^{-1} that is also not observed in the infrared or in the emission spectrum; more over, a related sideband upon the lower $^2A_1$ origin is missing;

(iv) Several lines can be reasonably explained as vibronic sidebands upon this zero-phonon transition, e.g. line 27 corresponds to $\nu_5(a_1)$.

Valuable assignments can also be given for peaks occuring in the higher energy region of 16700—19000 cm^{-1}, which have been detected by our special technique for measuring extremely weak features in absorption spectra (Fig. 3). The ν(C–N) and the symmetric and antisymmetric ν(N–H) modes appear at frequencies where they cannot interfere with any vibronic sideband originating in another electronic state. For example, the lines 37, 44, and 45, defying an assignment upon $^2E_g(O_h)$, clearly represent vibronic members of a split level of $^2T_{1g}(O_h)$ that turns out to be $^2A_2$ (cf. next section); due to vibrational energies of 2107, 3149, and 3334 cm^{-1}, assignments to the stretching modes σ(C–N), $\sigma(N–H)_s$, and $\sigma(N–H)_{as}$, respectively, are straightforward. These assignments are strongly supported by the observed deuterium shifts, which are significant only for those vibrational sidebands which involve some motion of the NH_3 groups (cf. Table 1).

The identification of the other two origins, i.e. the Γ_6, Γ_7 spin-orbit levels of $^2E(^2T_{1g})$, is more difficult. This is not unexpected, because the very detailed vibronic structure of the ^2E_g levels usually covers the much weaker zero-phonon lines of $^2T_{1g}$. However, a feature of the intense broad band 11 and the shoulder 12 can be pointed out as being candidates from the subsequent analysis of the remaining lines. All of the results of our spectroscopic analysis of the $^4A_{2g}\rightarrow{}^2E_g$, $^2T_{1g}$ transitions are summarized in Table 3.

AOM Calculations: A ligand field calculation of the full d^3 energy level scheme of a chromium(III) com-

Table 3. Absorption Frequencies (cm^{-1}) of $[Cr(CN)(NH_3)_5]Cl(ClO_4)$, $[Cr(CN)(NH_3)_5]Cl_2$ and $[Cr(CN)(ND_3)_5]Cl_2$ at 78 K

No.	$[Cl(ClO_4)]$		$[(Cl_2)]$	15-d$[(Cl_2)]$	Assignments
1	14717vs	σ	14675vs	14648vs	$^2A_1$
2	14831	σ	14800	14810	$^2A_1$+lattice
3	14908	π	14880	14864	$^2A_1+\delta$(N–Cr–N) [ν_9]
4	14952vs	σ,π	14918s	14927vs	$^2B_1$
5	14962	π	14925	14907	$^2A_1+\delta$(N–Cr–N) [ν_8]
6	14991	σ	14950		$^2A_1+\delta$(N–Cr–N) [ν_7]
7	15068vs	σ	15024s	15027s	$^2A_1+\delta$(Cr–C–N) [ν_6]
			15038s	15039s	$^2A_1+\sigma$(Cr–C–N) [ν_5]
8	15094	π			$^2B_1$+lattice
				15073	$^2A_1+\sigma$(Cr–N) [ν_3]
9	15153		15107	15084	$^2A_1+\sigma$(Cr–N) [ν_2]
10	15169		15143	15118	$^2E(\Gamma_7)$
11	15203bs	σ,π	15167bs	15150bs	$^2E(\Gamma_6)$
12	15222ssh	π	15190sh	15170	$^2B_1+\delta$(N–Cr–N) [ν_8]
13	15286	σ	15240	15230	$^2A_2$
			15263		$^2B_1+\delta$(Cr–C–N) [ν_6]
14	15303s	σ	15276		$^2B_1+\sigma$(Cr–C–N) [ν_5]
15	15344	σ	15306		$^2A_1+\rho(Cr–NH_3)$
16	15362		15330sh	15330vw	$^2B_1+\sigma$(Cr–N) [ν_3]
				15360	$^2B_1+\sigma$(Cr–N) [ν_1]
				15380	$^2A_2$+lattice
				15393	$^2A_1+\rho(Cr–NH_3)$
17	15394bs	π	15356bs	15200bs	$^2A_1+\rho(Cr–NH_3)$
18	15425	σ	15388	15370	$^2B_1+\sigma$(Cr–N) [ν_4]
19	15462b	σ,π	15424	15244	$^2A_1+\rho(Cr–NH_3)$
20	15475	σ		15273bs	$^2A_1+\rho(Cr–NH_3)$
21	15518	σ		15415	$^2A_2+\delta$(N–Cr–N) [ν_9]
22	15528	σ	15492	15475	$^2E(\Gamma_7)+\delta$(Cr–C–N) [ν_6]
23	15539	σ	15508	15432	$^2A_2+\delta$(N–Cr–N) [ν_8]
24	15560	σ	15528	15489	$^2E(\Gamma_6)+\delta$(Cr–C–N) [ν_6]
25	15579	σ	15470		$^2A_2+\delta$(N–Cr–N) [ν_7]
26	15628	π	15550	15350	$^2B_1+\rho(Cr–NH_3)$
27	15637	σ	15600	15602	$^2A_2+$(N–Cr–N) [ν_5]
28	15679ssh	π	15638bs	15489bs	$^2B_1+\rho(Cr–NH_3)$
29	15690bs	π	15661	15518bs	$^2B_1+\rho(Cr–NH_3)$
30	15750	σ,π	15720	15602	$^2A_1+\rho(Cr–NH_3)+[\nu_5]$
31	15870	σ			$^2E(\Gamma_7)+\rho(Cr–NH_3)$
32	15912	σ			$^2E(\Gamma_6)+\rho(Cr–NH_3)$
33	16557	#	16517		$^2B_1+\delta$(H–N–H)
34	16824spw	#	16786spw		$^2A_1+\sigma$(C–N)
35	17070spw	#	17037		$^2B_1+\sigma$(C–N)
36	17175spw	#	17134		$^2A_1+\sigma$(C–N)+[ν_5]
37	17393	#			$^2A_2+\sigma$(C–N)
38	17870	#			$^2A_1+\sigma$(N–H)
39	18052	#	18000	(17203)*	$^2A_1+\sigma$(N–H)
40	18109	#			$^2B_1+\sigma$(N–H)
41	18157	#	18103vw		$^2B_1+\sigma$(N–H)
42	18290	#	18199	(17437)*	$^2B_1+\sigma$(N–H)
43	18412	#	18370vw		$^2A_1+\sigma$(N–H)+[ν_5]
44	18435	#	18406vw		$^2A_2+\sigma$(N–H)
45	18620	#	18561vw	(17775)*	$^2A_2+\sigma$(N–H)

Polarizations are denoted by σ and/or π; #: measurements for powdered sample (see experimental section); vs: very strong, s: strong, bs: broad strong, b: broad, ssh: strong shoulder, spw: sharp weak, vw; very weak. *: data on 15-d$[Cl(ClO_4)]$.

plex leads to the diagonalization of a 120-dimensional secular determinant which arises from the perturbated d^3 system.[3] In the framework of the AOM, metal ligand interactions are described in terms of localized metal-ligand bonding parameters of the σ- and π-type. Therefore, in the case of a tetragonal pentaammine complex,

a total of at least six electronic parameters has to be considered: two Racah parameters (B and C) that describe the interelectronic repulsion; the quantity ζ accounts for the spin-orbit coupling; and the ligand field potential is set up by means of three AOM parameters ($e_\sigma(NH_3)$, $e_\sigma(CN)$, and $e_\pi(CN)$). The metal-ligand π-interaction with the ammonia ligands can be reasonably neglected, i.e. $e_\pi(NH_3)=0$. Although the structural parameters involved in an AOM calculation are known for the present complex from our X-ray investigation, one may be confronted with the problem of overparametrization, which can yield quite good fits of the energy-level scheme, even for some incorrect band assignments or unphysical parameter sets. On the other hand, since the (spherical) Racah parameters influence the low-symmetry level splittings considered here only to a small extent, these quantities can already be derived from the quartet band separation ($^4T_{1g}-{}^4T_{2g}$ corresponds ca. 12B) and from the position of the lowest doublet ($^2E_g-{}^4A_{2g}$ corresponds ca. 9B+3C).[10] Moreover, AOM parameters are usually transferable between similar compounds; particularly, $e_\sigma(NH_3)$ is well established from many calculations on similar ammine complexes to show values close to 7200 cm^{-1}.[11] Neglecting (to a good approximation) small effects of the spin-orbit coupling on the quartet states, low-symmetry ligand field splittings can be visualized by means of two-dimensional contour plots. This is illustrated in Fig. 6, showing that the experimental splitting of quartet bands (Fig. 1) are reproduced only if a negative value for $e_\pi(CN)$ is assumed. This clearly demonstrates the π acceptor property of the cyanide ligand, which is, indeed, not unexpected for cyano complexes of chromium(III).[7,8] However, due to some uncertaintities

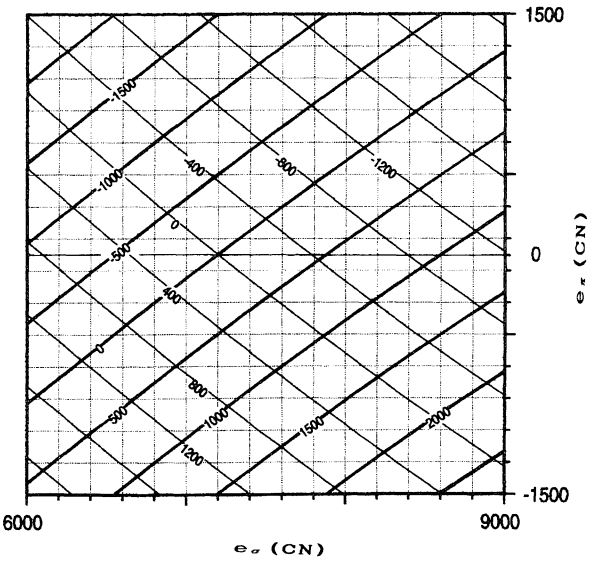

Fig. 6. Contour diagram for the level splittings of $^4T_{2g}$ ($^4E^a-{}^4B_2$: bold line) and $^4T_{1g}$ ($^4E^b-{}^4A_2$: thin line). Parameter values: $B=700$; $\zeta=0$, $e_\sigma(NH_3)=7200$, $e_\pi(NH_3)=0$; (in cm^{-1}).

involved in the band deconvolution procedure, we can not obtain a definite parameter value ($e_\pi(CN)$) from the quartet band splittings alone. We therefore need information concerning the ligand field states, which are available from the intercombination band region exhibiting well resolved band profiles in absorption and emission. In particular, a reasonable analysis of the vibronic structure leads to certain assignments for at least three of the five spin-orbit components of ^2E_g, $^2T_{1g}$, (cf. last section). On the other hand, it is known that the doublet splittings in tetragonal chromium(III) complexes can be crucially influenced by low-symmetry effects embodied in the interelectronic repulsion terms, which are inadequately described within the conventional ligand field theory.[4] In this field, the experimentally well-determined splitting of the lowest excited state (^2E_g) has been a particular subject of a series of detailed investigations on pentaammine complexes. However, Schmidtke et al.[7] have recently shown that the unusual large ^2E_g splittings can be reproduced only if a π-orbital expansion factor is included in the electronic repulsion part. The shortcoming of using spherical (!) Recah parameters in treating the interelectronic repulsion has already been discussed by Jørgensen,[19] who introduced several nephelauxetic ratios (β_{55}, β_{35}, $\cdots$) in order to account for the different electron-electron interactions. Since we are concerned here with pure spin-flip transitions within the $(t_{2g})^3$ electron configuration, and because NH_3 ligands do not contribute to π bonding, only one additional parameter is required for the present C_{4v} symmetry.[7] This orbital reduction factor $\tau=\tau_{xz}=\tau_{yz}<1$ considers interelectronic effects due to the π delocalization of metal-d electrons toward the axial CN ligand. Consequently, one more parameter has now to be included in the AOM calculations. On the other hand, relevant parameter space can be reduced by applying the familiar relation between the ligand field strength and the AOM parameters,

$$10Dq = 3e_\sigma - 4e_\pi, \tag{6}$$

since Dq(CN) is known from the octahedral $[Cr(CN)]^{3-}$ complex.[16] When using a reasonable value for the spin-orbit coupling constant (ζ), again no more than two parameters, i.e. the orbital expansion coefficient τ and either $e_\sigma(CN)$ or $e_\pi(CN)$, respectively, have to be varied freely in order to calculate the d–d transition energies for $[Cr(CN)(NH_3)_5]^{2+}$. Figure 7 shows such a two-dimensional contour diagram on the splitting of ^2E_g that illustrates the effect of the orbital expansion together with the influence of varying $e_\pi(CN)$. Obviously, the experimentally obtained value of 235 cm^{-1} can not be reproduced when the orbital expansion effect is ignored ($\tau=1$). Otherwise, the τ values close to 0.99 also lead to satisfactory results for the higher doublet states, as shown, for example, for the $^2A_2(^2T_{1g})-{}^2A_1(^2E_g)$ separation, which is included in this contour plot. This

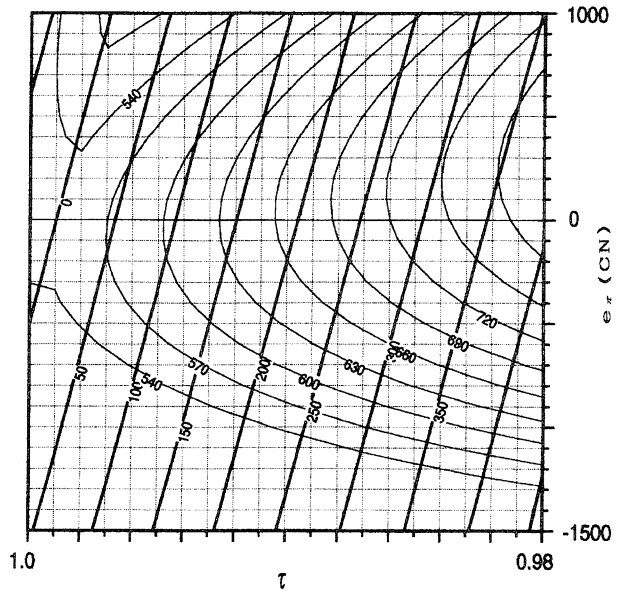

Fig. 7. Contour plot for the ^2E_g splitting (bold line) and for the energy difference between the highest spin-orbit level of $^2T_{1g}$ and the lower component of ^2E_g. Parameter values: $B=650$; $C=3400$, $\zeta=200$, $e_\sigma(NH_3)=7200$, $e_\pi(NH_3)=0$; (in cm^{-1}).

result is in excellent agreement with earlier results concerning other halogenopentaammines[4,6,7] of chromium(III). Considering the crossing point of the respective isolines, we obtain the parameter values $\tau=0.99$ and $e_\pi(CN)=-900$ cm^{-1} (Fig. 7), where the latter implies $e_\sigma(CN)=7566$ cm^{-1} from Eq. 6.

In order to check these results, we also performed some calculations on the energy-level scheme using a fitting routine based on the Powell algorithm.[3] This procedure yielded reasonable fits for all of the observed quartet and doublet energies, likewise, which is illustrated in Table 4. Although the final parameter values may be influenced to some extent by weighting factors that may be introduced in order to balance the spectral resolution for quartet and doublet transitions, we found the resulting AOM parameters to be *de facto* not dependent on a distinct set of starting parameters. In conclusion, our results show a σ-antibonding behavior, $e_\sigma(CN)$=ca. 7500 cm^{-1}, that exceeds not too much the ammonia ligand ($e_\sigma(NH_3)=7200$ cm^{-1}), together with strong π-acceptor interaction, $e_\pi(CN)$=ca. −900 cm^{-1}, summarizing both effects to the well-known very strong ligand field potential of the soft cyanide ligand. Vanquickenborne et. al.[8] have estimated the values of $e_\sigma(CN)=8480$ cm^{-1} and $e_\pi(CN)=-290$ cm^{-1} based only on the qurtet band splittings found in the solution spectra of aquacyano-complexes of chromium(III) repoted by Perumareddi.[18] However, the parameter values given here appear to be rather significant, as deduced on the basis of a manifold of quartet and doublet transitions which were obtained from highly resolved single-crystal absorption spectra.

Table 4. Observed and Calculated Energy Levels in $[Cr(CN)(NH_3)_5]^{2+}$

Energy level	Expt	Cacld	Dev.
$^2A_1(\Gamma_7)$	14717	14722	5
$^2B_1(\Gamma_6)$	14952	14952	0
$^2E_g(O_h)$ split	235	230	−5
$^2E^a(\Gamma_7)$	15169	15144	−25
$^2E^b(\Gamma_6)$	15203	15182	−21
$^2A_2(\Gamma_6)$	15286	15247	−39
$^2T_{1g}(O_h)-{}^2E_g(O_h)$	569	525	−44
$^4B_2$	ca. 21600	21600	0
$^4E^a$	ca. 22280	23200	920
$^4T_{2g}(O_h)$ split	ca. 680	1600	920
$^4A_2$	ca. 28100	28350	250
$^4E^b$	ca. 29050	28950	−100
$^4T_{1g}(O_h)$ split	ca. 950	600	−350

Optimized parameters: $e_\sigma(CN)=7480$, $e_\pi(CN)=-890$, $B=610$, $C=3515$, $\tau=0.99$. Fixed values: $Dq(CN)=2600$, $\zeta=230$, $e_\sigma(NH_3)=7200$, $e_\pi(NH_3)=0$; all in cm^{-1}.

We thank G. Nierhauve, University of Düsseldorf, for measuring the resonant emission spectrum of $[Cr(CN)(NH_3)_5]Cl(ClO_4)$. One of us (TS) appreciates financial support from the Deutsche Forschungsgemeinschaft, Bonn.

References

1) H. L. Schläfer, *Z. Elektrochem.*, **64**, 887 (1960).
2) L. S. Forster, J. V. Rund, and A. F. Fucularo, *J. Phys. Chem.*, **88**, 5012 (1984).
3) P. E. Hoggard, *Coord. Chem. Rev.*, **70**, 85 (1986).
4) C. D. Flint and A. P. Matthews, *J. Chem. Soc., Faraday Trans. 2*, **69**, 419 (1973).
5) S. Decurtins, H. U. Güdel, and K. Neuenschwander, *Inorg. Chem.*, **16**, 796 (1977).
6) T. Schöherr and H. -H. Schmidtke, *Inorg. Chem.*, **18**, 2726 (1979).
7) H. -H. Schmidtke, H. Adamsky, and T. Schönherr, *Bull. Chem. Soc. Jpn.*, **61**, 59 (1988).
8) L. G. Vanquickenborne and A. Ceulemans, *Coord. Chem. Rev.*, **48**, 159 (1983).
9) P. Riccierei and E. Zinato, *Inorg. Chem.*, **19**, 853 (1980).
10) T. Schönherr and J. Degen, *Z. Naturforsch., A*, **45a**, 161 (1990).
11) T. Schönherr, "Applications of the Angular Overlap Model," in "Topics in Current Chemistry," ed by H. Yersin, Springer, Berlin, to be published.
12) T. Schönherr, R. Wiskemann, and D. Mootz, *Inorg. Chim. Acta*, **221**, 85 (1994).
13) A. Urushiyama, T. Schönherr, and H. -H. Schmidtke, *Ber. Bunsenges. Phys. Chem.*, **90**, 1188 (1986).
14) A. T. C. North, D. C. Phillips, and F. S. Mathews, *Acta Crystallogr., Sect. A*, **A24**, 351 (1968).
15) E. B. Wilson, J. C. Decius, and P. C. Cross, "Molecular Vibrations," McGraw-Hill, New York (1955).
16) T. Shimanouchi, "Center News," Computer Center of

University of Tokyo, Tokyo (1976), Vol. 6, p. 97.
17) A. B. P. Lever, "Inorganic Electronic Spectroscopy," 2nd ed, Elsevier, Amsterdam (1984).
18) J. R. Perumareddi, *Coord. Chem. Rev.*, **4**, 73 (1969).
19) C. K. Jørgensen; "Modern Aspects of Ligand Field Theory," North Holland, Amsterdam (1971).